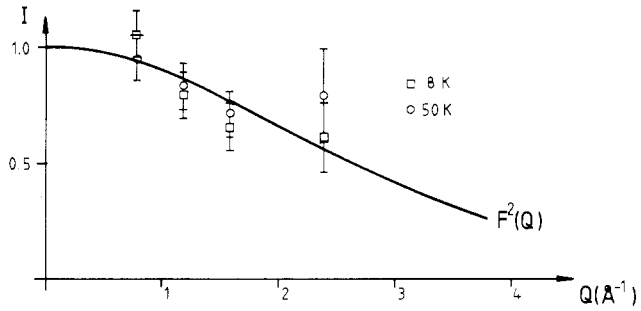

Figure 8. Q dependence of intensity of the magnetic transition at 31.6 cm^{-1} in fully deuteriated nickelocene measured at 6.8 and 50 K. For the plotted function the magnetic form factor $F(\vec{Q})$ was taken from ref 26.

therefore a too large value of susceptibility is measured, leading to a smaller value of D.

The intensity of the band at 31.6 ± 1.0 cm^{-1} in the INS experiments decreases as $F^2(Q)$ with increasing Q (Figure 8). This evidence proves the magnetic nature of this transition. Furthermore, the decrease in intensity of the magnetic transition on increasing temperature in Figure 7 is in qualitative agreement with what is expected on the basis of relative Boltzmann populations of the singlet and triplet levels. Estimating the intensity of the magnetic transition at high temperature is rather difficult because of the underlying elastic scattered neutrons.

There is a slight discrepancy between the zero-field splitting D_0 found from susceptibility measurements and the energy difference ΔE measured by INS. This is probably due to the different samples, since the INS experiments were performed with undiluted nickelocene with deuteriated ligands. The observed magnetic transition at 31.6 cm^{-1} in the INS spectra does not correspond to the zero-field splitting of an isolated molecule D_0 but will show some influence of the intermolecular coupling. One might think of the excited level of the triplet ground state in the undiluted sample as being a band of levels due to intermolecular coupling, the center of which need not be at the same energy level as in the isolated molecule.

6. Concluding Remarks

By introduction of two molecular fields describing the intermolecular interaction in undiluted nickelocene, we interpret the magnetic susceptibility of this compound, undiluted and doped into an isostructural diamagnetic host, by the *same* spin-Hamiltonian parameters. Furthermore the results of susceptibility measurements and INS investigations are in good agreement, confirming our approach. The accuracy of the zero-field-splitting parameter D_0 determined from susceptibility measurements is unique.

We have also shown the advantage of measuring the magnetic susceptibility on an oriented powder sample. Of course, one can only use this technique if the crystal structure of the compound investigated is known and the preferred orientation is almost perfect, as in our experiments. In most cases the orientation will be partial only, and a straightforward interpretation of such a measurement will be impossible. Anyway, the unwelcome effect of a spontaneous orientation of crystallites with anisotropic magnetic susceptibility should never be underestimated, and samples for isotropic powder measurements in a magnetic field have to be mechanically fixed. This may be performed as reported earlier.[19]

Acknowledgment. This work was supported by the Swiss National Science Foundation (Project 2.442.0.82). We thank Prof. Dr. J. H. Ammeter for helpful discussion.

Registry No. $Ni(C_5H_5)_2$, 1271-28-9; $Ni(C_5D_5)_2$, 51510-35-1.

(26) Watson, R. E.; Freeman, A. J. *Acta Crystallogr.* **1961**, *14*, 27.
(27) Prins, R.; van Voorst, J. D. W. *J. Chem. Phys.* **1968**, *49*, 4665.

Contribution from the Department of Chemistry, University of California, Irvine, California 92717

Bis(nitroxyl) Adducts of Cobalt and Nickel Hexafluoroacetylacetonates. Preparation, Structures, and Magnetic Properties of $M(F_6acac)_2(proxyl)_2$[1] (M = Co^{2+}, Ni^{2+})

Leigh C. Porter, Michael H. Dickman, and Robert J. Doedens*

Received July 27, 1987

Bisadducts of the cyclic nitroxyl radical 2,2,5,5-tetramethylpyrrolidinyl-1-oxy (proxyl) with nickel(II) and cobalt(II) hexafluoroacetylacetonates have been prepared and characterized by crystal structure analyses and magnetic susceptibility studies. The adducts are isostructural, each having a centrosymmetric molecular structure and a slightly distorted octahedral configuration about the metal ion. The O-bound nitroxyls adopt a trans configuration. Magnetic susceptibility data (6–300 K) indicate that antiferromagnetic coupling of ligand and metal free spins yields an $S = {}^1/_2$ ground state for M = Co^{2+} and an $S = 0$ ground state for M = Ni^{2+}. At higher temperatures, there is some population of excited states with greater spin multiplicities. Possible orbital interactions that could account for the magnetic behavior are discussed. Crystal data for $Co(F_6acac)_2(proxyl)_2$: monoclinic, space group $P2_1/c$, $Z = 2$, $a = 10.339$ (4) Å, $b = 14.533$ (4) Å, $c = 11.973$ (4) Å, $\beta = 111.09$ (2)°. Least-squares refinement based upon 1615 data with $F_o^2 > 3\sigma(F_o^2)$ and $2\theta \leq 50°$ converged to $R = 0.056$. Crystal data for $Ni(F_6acac)_2(proxyl)_2$: monoclinic, space group $P2_1/c$, $Z = 2$, $a = 10.243$ (5) Å, $b = 14.564$ (5) Å, $c = 11.902$ (5) Å. Least-squares refinement based upon 1609 nonzero data with $2\theta \leq 45°$ converged to $R = 0.052$.

Introduction

There has been increasing interest in compounds that contain one or more nitroxyl radicals coordinated to a transition-metal ion.[2-20] Such systems have been shown to exhibit diverse types of magnetic behavior, including antiferromagnetic and ferromagnetic exchange of varying magnitudes, diamagnetism, and

(1) Abbreviations for ligand names used in this paper include the following: tempo = 2,2,6,6-tetramethylpiperidinyl-1-oxy; proxyl = 2,2,5,5-tetramethylpyrrolidinyl-1-oxy; nitphen = 2-phenyl-4,4,5,5-tetramethylimidazoline-1-oxyl 3-oxide; F_6acac = hexafluoroacetylacetonato.
(2) Richman, R. M.; Kuechler, T. C.; Tanner, S. P.; Drago, R. S. *J. Am. Chem. Soc.* **1977**, *99*, 1055–1058.
(3) Drago, R. S.; Kuechler, T. C.; Kroeger, M. *Inorg. Chem.* **1979**, *18*, 2337–2342.
(4) Anderson, O. P.; Kuechler, T. C. *Inorg. Chem.* **1980**, *19*, 1417–1422.
(5) Dickman, M. H.; Doedens, R. J. *Inorg. Chem.* **1981**, *20*, 2677–2681 and references therein.
(6) Laugier, J.; Ramasseul, R.; Rey, P.; Espie, J. C.; Rassat, A. *Nouv. J. Chim.* **1983**, *7*, 11–14.
(7) Grand, A.; Rey, P.; Subra, R. *Inorg. Chem.* **1983**, *22*, 391–394.
(8) Porter, L. C.; Dickman, M. H.; Doedens, R. J. *Inorg. Chem.* **1983**, *22*, 1962–1964.
(9) Benelli, C.; Gatteschi, D.; Zanchini, C. *Inorg. Chem.* **1984**, *23*, 798–800.
(10) Bencini, A.; Benelli, C.; Gatteschi, D.; Zanchini, C. *J. Am. Chem. Soc.* **1984**, *106*, 5813–5818.
(11) Beck, W. *Inorg. Chim. Acta* **1985**, *99*, L33.
(12) Porter, L. C.; Doedens, R. J. *Inorg. Chem.* **1985**, *24*, 1006–1010.

0020-1669/88/1327-1548$01.50/0

simple paramagnetism. Factors that determine the nature and magnitude of the magnetic coupling in these systems include the metal coordination geometry, the metal–ligand distances, and the electronic structures of the metal and ligand. Qualitative correlations between these factors and magnetic behavior are emerging, but many of the details are not yet well-understood. A full understanding of the factors influencing the magnetic properties of these discrete molecular systems could help to provide a basis for development of extended systems with unusual magnetic or electrical properties.

Recently we reported the synthesis and characterization of bisadducts of the stable nitroxyl radicals tempo and proxyl with bis(hexafluoroacetylacetonato)manganese(II).[15] These were the first well-characterized molecules that contained two nitroxyl radicals bound to a single transition-metal center and proved to have interesting magnetic properties. At low temperatures (ca. 6–150 K), they behaved like $S = {}^3/_2$ systems but their magnetic susceptibilities at higher temperatures indicated population of one or more states of higher spin multiplicity in addition to the ground-state spin quartet. The experimental susceptibility curve could be closely fit by values calculated from a spin-only model for antiferromagnetic coupling of ligand ($S = {}^1/_2$) and metal ($S = {}^5/_2$) free spins. Subsequent solid-state EPR experiments yielded results consistent with the energy level pattern derived from the susceptibility data.[16]

We now report the preparation, structure, and magnetic properties of the analogous Co(II) and Ni(II) adducts of the proxyl radical.

Experimental Section

Synthesis. (a) Starting Materials. $Co(F_6acac)_2$ was prepared from the metal acetate by a standard procedure.[21] $Ni(F_6acac)_2$ was prepared by the addition of an equimolar amount of nickel(II) chloride to a 1.0 M solution of F_6acac in 1.0 M aqueous NaOH. The insoluble $Ni(F_6acac)_2$ that formed was isolated by filtration and dehydrated by azeotropic distillation with toluene. The ligand proxyl was prepared by the previously described method.[15]

(b) $Ni(F_6acac)_2(proxyl)_2$. The nickel adduct was prepared by the addition of 0.53 g (0.011 mol) of anhydrous $Ni(F_6acac)_2$ to a solution of 0.33 g (0.023 mol) of proxyl in pentane. The deep green solution that formed immediately was refluxed for 1 h under N_2, cooled, and filtered to remove unreacted starting material. Well-formed, somewhat air-sensitive dark green crystals formed when the solution was allowed to stand overnight at −20 °C. Anal. Calcd for $C_{26}H_{34}N_2O_6F_{12}Ni$: C, 41.27; H, 4.50; N, 3.70. Found: C, 41.10; H, 4.52; N, 3.67.

(c) $Co(F_6acac)_2(proxyl)_2$. The procedure was similar to that for the Ni complex, with the exception that heptane was used as a solvent. Deep red crystals formed when the reaction solution was allowed to stand overnight at room temperature. Anal. Calcd for $C_{26}H_{34}N_2O_6F_{12}Co$: C, 41.23; H, 4.52; F, 30.10. Found: C, 41.51; H, 4.43; F, 29.98.

Collection and Reduction of X-ray Data. Crystallographic data for both adducts were collected on a Syntex $P2_1$ diffractometer. Crystals were mounted on glass fibers and coated with a thin layer of spray lacquer (Co complex) or epoxy cement (Ni adduct) to retard decomposition. Initial centering, generation of possible unit cell vectors, and assignment of indices were carried out by procedures that have been described elsewhere.[22,23] Refined unit cell parameters were obtained from least-squares refinement based upon the setting angles of 15 reflections with $30° \le 2\theta \le 35°$. Intensities of four standard reflections were measured at regular intervals. Reflections whose intensities exceeded the valid range of the coincidence correction were remeasured at a lower filament current. The p factor in the expression[24] for the standard deviations of the observed intensities was assigned a value of 0.05. The data were corrected for standard decay, Lorentz, and polarization effects. No absorption corrections were made. All computations were carried out with a locally modified version of the UCLA Crystallographic Computing Package.[25] Crystal data and experimental parameters for both compounds are tabulated in Table I.

Table I. Crystal Data and Experimental Parameters for $M(F_6acac)_2(proxyl)_2$

	M = Co	M = Ni
	(a) Crystal Data	
formula	$CoC_{26}H_{34}F_{12}N_2O_6$	$NiC_{26}H_{34}F_{12}N_2O_6$
fw	757.47	757.24
a, Å	10.339 (4)	10.243 (5)
b, Å	14.533 (4)	14.564 (5)
c, Å	11.973 (4)	11.902 (5)
β, deg	111.09 (2)	110.87 (3)
vol, Å^3	1678.5 (9)	1659.0 (11)
Z	2	2
d(calcd), g/cm^3	1.50	1.52
space group	$P2_1/c$	$P2_1/c$
μ(Mo Kα), cm^{-1}	6.1	6.9
	(b) Experimental Parameters	
radiation	Mo Kα; λ(Kα) = 0.71073 Å; graphite monochromator	
temp, °C	25	23
scan rate, deg/min	4–15	2–12
scan range, deg	−1.1 from Kα_1 to +1.2 from Kα_2	
bkgd counting	evaluated from 96-step peak profile	
2θ(max), deg	50	45
no. of data collected	2970 ($h,k,\pm l$)	2420 ($h,k,\pm l$)
no. of data with $F_o^2 > 3\sigma(F_o^2)$	1615	1609

Interaxial angles and axial rotation photographs indicated that both compounds crystallize in the monoclinic system. Systematic absences ($h0l$, $l \neq 2n$; $0k0$, $k \neq 2n$) uniquely define the space group $P2_1/c$, and a reasonable calculated density is obtained for $Z = 2$ molecules per unit cell. This implies a centrosymmetric molecular structure with the metal atom at the cell origin.

Intensity data for the Ni complex were obtained from a well-formed crystal of approximate dimensions 0.5 × 0.5 × 0.5 mm. The standard reflections declined in intensity by an average of about 10% during data collection; a correction was applied for this decay. The crystal of the Co adduct was triangular in shape, with dimensions 0.2 × 0.3 × 0.5 mm. The decline of the intensities of the standard reflections was less than 2%, and no decay correction was applied.

Structure Solution and Refinement. Both structures were solved by heavy-atom methods with the metal atom placed at the cell origin. The final refinement model included anisotropic thermal parameters for all non-hydrogen atoms. Hydrogen atoms were included at fixed, idealized positions but were not refined. Calculated positions of methyl hydrogen atoms were based on peaks observed on a difference Fourier map, except in the case of C(6) of the Co adduct, for which no acceptable methyl hydrogen peaks were found. In all refinements, the function minimized was $\sum w(|F_o| - |F_c|)^2$ and atomic scattering factors were taken from ref 26.

Final refinement for the Co adduct converged to conventional R factors $R_1 = 0.056$ and $R_2 = 0.070$. The final esd of an observation of unit weight was 1.85, and the largest peak height on a final difference Fourier map was 0.95 e/Å^3. For the Ni adduct, the final R factors were 0.052 and 0.068 and the esd of an observation of unit weight was 2.05. The height of the largest peak on a final difference map was 1.19 e/Å^3.

Magnetic Susceptibility Measurements. Magnetic susceptibility data were obtained for $T = 6$–300 K at 10 T by use of an SHE Corp. SQUID magnetometer located at the University of Southern California. Data were corrected for magnetization of the sample holder and for ligand diamagnetism, estimated from Pascal's constants. The susceptibility values were converted to effective magnetic moments by the expression

(13) Benelli, C.; Gatteschi, D.; Carnegie, D. W.; Carlin, R. L. *J. Am. Chem. Soc.* **1985**, *107*, 2560–2561.
(14) Porter, L. C.; Dickman, M. H.; Doedens, R. J. *Inorg. Chem.* **1986**, *25*, 678–684.
(15) Dickman, M. H.; Porter, L. C.; Doedens, R. J. *Inorg. Chem.* **1986**, *25*, 2595–2599.
(16) Benelli, C.; Gatteschi, D.; Zanchini, C.; Doedens, R. J.; Dickman, M. H.; Porter, L. C. *Inorg. Chem.* **1986**, *25*, 3453–3457.
(17) Laugier, J.; Rey, P.; Benelli, C.; Gatteschi, D.; Zanchini, C. *J. Am. Chem. Soc.* **1986**, *108*, 6931–6937.
(18) Felthouse, T. R.; Dong, T.-Y.; Hendrickson, D. N.; Shieh, H.-S.; Thompson, M. R. *J. Am. Chem. Soc.* **1986**, *108*, 8201–8214.
(19) Gatteschi, D.; Laugier, J.; Rey, P.; Zanchini, C. *Inorg. Chem.* **1987**, *26*, 938–943.
(20) Caneschi, A.; Gatteschi, D.; Laugier, J.; Rey, P. *J. Am. Chem. Soc.* **1987**, *109*, 2191–2192.
(21) Cotton, F. A.; Holm, R. H. *J. Am. Chem. Soc.* **1960**, *82*, 2979–2983.
(22) Churchill, M. R.; Lashewycz, R. A.; Rotella, F. J. *Inorg. Chem.* **1977**, *16*, 265–271.
(23) Sams, D. B.; Doedens, R. J. *Inorg. Chem.* **1979**, *18*, 153–156.
(24) Corfield, P. W. R.; Doedens, R. J.; Ibers, J. A. *Inorg. Chem.* **1967**, *6*, 197–204.
(25) Strouse, C. E., personal communication.
(26) *International Tables for X-ray Crystallography*; Kynoch: Birmingham, England, 1974; Vol. 4.

Table II. Positional Parameters for Non-Hydrogen Atoms of $Co(F_6acac)_2(proxyl)_2$

atom	x	y	z
Co	0.0000	0.0000	0.0000
O(1)	0.1690 (4)	0.0512 (3)	−0.0443 (4)
O(2)	−0.0758 (4)	0.1280 (3)	0.0141 (3)
O(3)	−0.1402 (4)	−0.0072 (3)	−0.1701 (3)
N	0.1906 (5)	0.0918 (4)	−0.1308 (4)
C(1)	0.2311 (7)	0.1893 (5)	−0.1229 (6)
C(2)	0.2871 (12)	0.1966 (7)	0.2218 (9)
C(3)	0.2527 (11)	0.1170 (7)	−0.2941 (8)
C(4)	0.2198 (7)	0.0401 (5)	−0.2260 (6)
C(5)	0.1079 (10)	0.2499 (6)	−0.1360 (11)
C(6)	0.3432 (9)	0.2077 (6)	−0.0031 (8)
C(7)	0.0901 (9)	−0.0128 (7)	−0.2992 (8)
C(8)	0.3428 (9)	−0.0257 (6)	−0.1680 (9)
C(9)	−0.1866 (6)	0.1607 (4)	−0.0584 (5)
C(10)	−0.2709 (6)	0.1256 (4)	−0.1667 (5)
C(11)	−0.2408 (6)	0.0452 (5)	−0.2146 (5)
C(12)	−0.2280 (7)	0.2518 (5)	−0.0170 (7)
C(13)	−0.3409 (7)	0.0132 (6)	−0.3369 (6)
F(1)	−0.3367 (6)	0.2901 (4)	−0.0924 (5)
F(2)	−0.1316 (5)	0.3129 (3)	0.0063 (6)
F(3)	−0.2504 (8)	0.2445 (4)	0.0812 (6)
F(4)	−0.2791 (4)	−0.0016 (4)	−0.4113 (4)
F(5)	−0.4414 (4)	0.0717 (4)	−0.3879 (4)
F(6)	−0.4005 (6)	−0.0633 (4)	−0.3287 (4)

Table III. Positional Parameters for Non-Hydrogen Atoms of $Ni(F_6acac)_2(proxyl)_2$

atom	x	y	z
Ni	0.0000	0.0000	0.0000
O(1)	−0.1713 (4)	−0.0482 (3)	0.0407 (4)
O(2)	0.0726 (4)	−0.1267 (2)	−0.0161 (3)
O(3)	0.1354 (4)	0.0085 (3)	0.1689 (3)
N	−0.1913 (5)	−0.0897 (3)	−0.1294 (4)
C(1)	−0.2197 (7)	−0.0390 (5)	0.2258 (6)
C(2)	−0.2554 (11)	−0.1153 (7)	0.2921 (8)
C(3)	−0.2887 (11)	−0.1961 (6)	0.2181 (9)
C(4)	−0.2297 (7)	−0.1883 (5)	0.1211 (6)
C(5)	−0.0928 (9)	0.0158 (7)	0.2983 (8)
C(6)	−0.3414 (10)	0.0256 (6)	0.1690 (8)
C(7)	−0.3400 (9)	−0.2064 (6)	0.0008 (8)
C(8)	−0.1061 (10)	−0.2473 (6)	0.1356 (11)
C(9)	0.1834 (6)	−0.1597 (4)	0.0568 (5)
C(10)	0.2682 (6)	−0.1246 (4)	0.1666 (5)
C(11)	0.2377 (6)	−0.0442 (5)	0.2135 (5)
C(12)	0.2261 (8)	−0.2502 (5)	0.0164 (7)
C(13)	0.3366 (7)	−0.0118 (5)	0.3365 (6)
F(1)	0.3341 (6)	−0.2893 (3)	0.0927 (5)
F(2)	0.1281 (5)	−0.3116 (3)	−0.0087 (6)
F(3)	0.2502 (8)	−0.2425 (4)	−0.0816 (6)
F(4)	0.3970 (6)	0.0643 (4)	0.3274 (4)
F(5)	0.4388 (4)	−0.0700 (3)	0.3883 (4)
F(6)	0.2739 (5)	0.0025 (4)	0.4112 (4)

Table IV. Bond Distances (Å) in $Co(F_6acac)_2(proxyl)_2$[a]

(a) Co Coordination Sphere			
Co–O(1)	2.134 (4)	Co–O(3)	2.033 (4)
Co–O(2)	2.050 (4)		
(b) F_6acac Ligand			
O(2)–C(9)	1.255 (6)	C(10)–C(11)	1.385 (8)
C(9)–C(10)	1.374 (8)	C(11)–C(13)	1.530 (8)
C(9)–C(12)	1.529 (9)	C(11)–O(3)	1.244 (7)
(c) Proxyl Ligand			
O(1)–N	1.279 (6)	C(1)–C(6)	1.508 (10)
N–C(1)	1.472 (8)	C(2)–C(3)	1.412 (12)
N–C(4)	1.485 (8)	C(3)–C(4)	1.493 (10)
C(1)–C(2)	1.497 (10)	C(4)–C(7)	1.520 (10)
C(1)–C(5)	1.509 (11)	C(4)–C(8)	1.542 (10)

[a] Distances within the CF_3 groups are included with the supplementary material.

$\mu_{eff} = 2.828(\chi_m T)^{1/2}$. In the case of the nickel complex, a correction of 180×10^{-6} cm^3/mol was applied for the temperature-independent paramagnetism of the Ni atom.

Table V. Bond Distances (Å) in $Ni(F_6acac)_2(proxyl)_2$[a]

(a) Ni Coordination Sphere			
Ni–O(1)	2.100 (4)	Ni–O(3)	1.998 (4)
Ni–O(2)	2.024 (4)		
(b) F_6acac Ligand			
O(2)–C(9)	1.253 (6)	C(10)–C(11)	1.380 (8)
C(9)–C(10)	1.384 (8)	C(11)–C(13)	1.528 (8)
C(9)–C(12)	1.520 (9)	C(11)–O(3)	1.254 (7)
(c) Proxyl Ligand			
O(1)–N	1.295 (6)	C(1)–C(6)	1.515 (10)
N–C(1)	1.478 (8)	C(2)–C(3)	1.436 (11)
N–C(4)	1.483 (8)	C(3)–C(4)	1.486 (10)
C(1)–C(2)	1.482 (12)	C(4)–C(7)	1.498 (10)
C(1)–C(5)	1.507 (10)	C(4)–C(8)	1.488 (11)

[a] Distances within the CF_3 groups are included with the supplementary material.

Table VI. Bond Angles (deg) in $Co(F_6acac)_2(proxyl)_2$[a]

(a) Co Coordination Sphere			
O(1)–Co–O(2)	94.3 (2)	O(2)–Co–O(3)	88.5 (2)
O(1)–Co–O(3)	97.0 (2)		
(b) F_6acac Ligand			
Co–O(2)–C(9)	124.6 (4)	C(9)–C(10)–C(11)	122.9 (5)
Co–O(3)–C(11)	125.6 (4)	O(3)–C(11)–C(10)	128.1 (6)
O(2)–C(9)–C(10)	128.6 (6)	O(3)–C(11)–C(13)	113.4 (6)
O(2)–C(9)–C(12)	113.3 (5)	C(10)–C(11)–C(13)	118.5 (5)
C(10)–C(9)–C(12)	118.1 (5)		
(c) Proxyl Ligand			
Co–O(1)–N	139.4 (4)	C(5)–C(1)–C(6)	109.0 (7)
O(1)–N–C(1)	121.4 (5)	C(1)–C(2)–C(3)	110.1 (7)
O(1)–N–C(4)	122.2 (5)	C(2)–C(3)–C(4)	109.6 (7)
C(1)–N–C(4)	113.9 (5)	N–C(4)–C(3)	101.0 (6)
N–C(1)–C(2)	101.5 (6)	N–C(4)–C(7)	108.5 (6)
N–C(1)–C(5)	110.2 (6)	N–C(4)–C(8)	109.3 (6)
N–C(1)–C(6)	109.6 (6)	C(3)–C(4)–C(7)	113.0 (8)
C(2)–C(1)–C(5)	115.4 (8)	C(3)–C(4)–C(8)	113.4 (7)
C(2)–C(1)–C(6)	110.8 (7)	C(7)–C(4)–C(8)	111.1 (7)

[a] Bond angles within the CF_3 groups are included with the supplementary material.

Table VII. Bond Angles (deg) in $Ni(F_6acac)_2(proxyl)_2$[a]

(a) Ni Coordination Sphere			
O(1)–Ni–O(2)	94.7 (2)	O(2)–Ni–O(3)	90.3 (2)
O(1)–Ni–O(3)	97.2 (2)		
(b) F_6acac Ligand			
Ni–O(2)–C(9)	123.8 (4)	C(9)–C(10)–C(11)	122.6 (5)
Ni–O(3)–C(11)	124.3 (4)	O(3)–C(11)–C(10)	128.6 (5)
O(2)–C(9)–C(10)	128.4 (6)	O(3)–C(11)–C(13)	112.7 (6)
O(2)–C(9)–C(12)	113.9 (5)	C(10)–C(11)–C(13)	118.8 (6)
C(10)–C(9)–C(12)	117.7 (5)		
(c) Proxyl Ligand			
Ni–O(1)–N	137.1 (4)	C(5)–C(1)–C(6)	109.3 (7)
O(1)–N–C(1)	122.1 (5)	C(1)–C(2)–C(3)	109.7 (7)
O(1)–N–C(4)	120.9 (5)	C(2)–C(3)–C(4)	109.9 (7)
C(1)–N–C(4)	114.5 (5)	N–C(4)–C(3)	101.2 (6)
N–C(1)–C(2)	101.1 (6)	N–C(4)–C(7)	109.0 (6)
N–C(1)–C(5)	109.9 (6)	N–C(4)–C(8)	110.9 (6)
N–C(1)–C(6)	108.8 (6)	C(3)–C(4)–C(7)	110.6 (7)
C(2)–C(1)–C(5)	114.7 (7)	C(3)–C(4)–C(8)	115.5 (8)
C(2)–C(1)–C(6)	112.5 (7)	C(7)–C(4)–C(8)	109.3 (7)

[a] Bond angles within the CF_3 groups are included with the supplementary material.

Results

Crystal Structures. Final atomic coordinates for the Co and Ni complexes are tabulated in Tables II and III, respectively. Bond distances and angles are listed in Tables IV–VII. Available as supplementary material are tables of observed and calculated structure factors, anisotropic thermal parameters, hydrogen atom coordinates, distances and angles within the CF_3 groups, and least-squares planes.

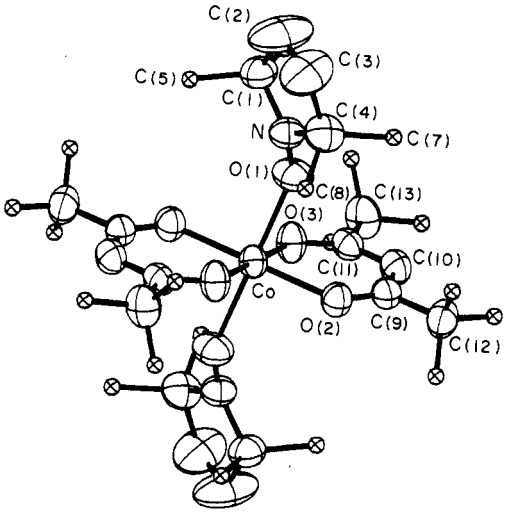

Figure 1. View of the molecular structure of $Co(F_6acac)_2(proxyl)_2$. For clarity, fluorine atoms and methyl carbon atoms have been given artificially small thermal parameters. Other thermal ellipsoids are drawn at the 50% probability level.

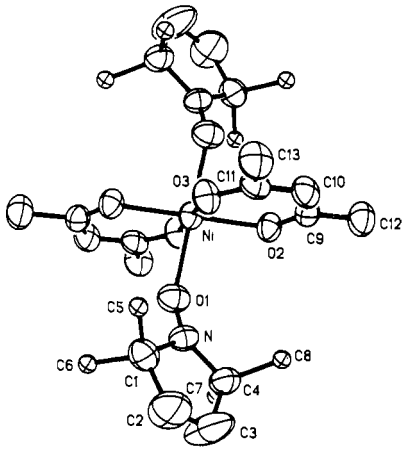

Figure 2. View of the molecular structure of $Ni(F_6acac)_2(proxyl)_2$. For clarity, fluorine atoms have been omitted and methyl carbon atoms have been given artificially small thermal parameters. Other thermal ellipsoids are drawn at the 50% probability level.

Description of the Structures. The bis(proxyl) adducts of cobalt(II) and nickel(II) hexafluoroacetylacetonates are isomorphous and isostructural with each other and with their previously reported manganese(II) analogue.[15] In both molecules, the metal atom is bound to two chelating F_6acac ligands and two nitroxyls in a centrosymmetric trans-octahedral configuration. Views of the molecular structures are shown in Figures 1 and 2.

The principal angular distortion from regular octahedral symmetry about the metal ions involves deviations of 4–7° of the metal–O(nitroxyl) bond from perpendicularity to the plane defined by the two metal–F_6acac bonds. In both adducts, the metal–O(nitroxyl) bond distances are longer by 0.08–0.10 Å than the metal–O(F_6acac) distances. In conformity with general atomic size trends, the Ni–O bonds are uniformly shorter (by ca. 0.03 Å) than the corresponding Co–O bonds. In both adducts, the carbon and oxygen atoms of the chelating F_6acac ligands are coplanar and the metal atom is about 0.29 Å out of the chelate plane. Other structural details of the chelating ligands are much as expected.

The nitroxyl radical is bound in a monodentate fashion through its oxygen atom. The Co–O and Ni–O distances (2.134 (4) and 2.100 (4) Å) are slightly shorter than the Mn–O distance of 2.150 (4) Å in the analogous manganese complex. The M–O–N angles of 139.4 (4)° (M = Co) and 137.1 (4)°, (M = Ni) are also smaller than the corresponding value of 145.3 (4)° in the manganese adduct. The N–O distances (1.279 (6) Å for M = Co^{2+} and 1.295 (6) Å for M = Ni^{2+}), together with the out-of-plane displacement

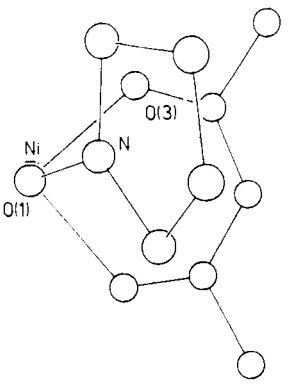

Figure 3. Schematic view of the asymmetric unit of the nickel adduct projected approximately down the O–Ni bond. This view is meant to show the orientation of the N–O bond relative to the equatorial Ni–O bonds.

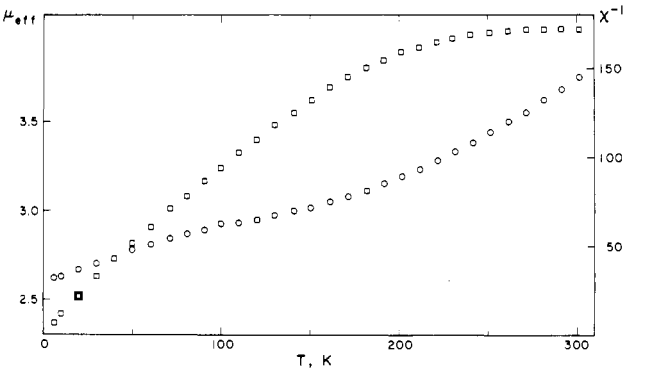

Figure 4. Inverse magnetic susceptibility (squares) and effective magnetic moment (circles) vs T for $Co(F_6acac)_2(proxyl)_2$.

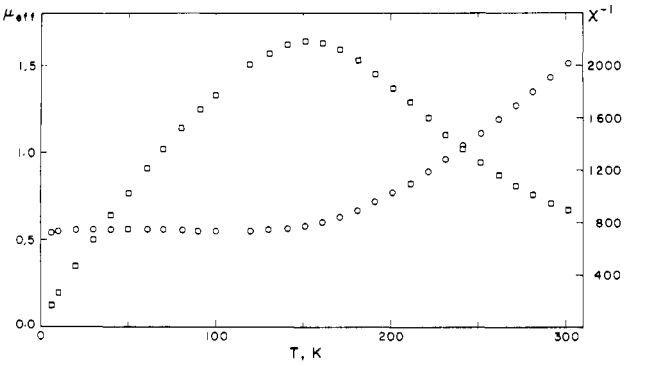

Figure 5. Inverse magnetic susceptibility (squares) and effective magnetic moment (circles) vs T for $Ni(F_6acac)_2(proxyl)_2$.

of the nitrogen atom (0.13 Å in both adducts), are typical for nitroxyl radicals of this type.[27,28] As has been found in other proxyl adducts, the thermal ellipsoids of C(2) and C(3) are suggestive of some stereochemical flexibility and/or disorder in the solid state. Other structural features of the nitroxyl ligands are unexceptional.

As is illustrated in Figure 3, the N–O(1) and metal–O(3) bonds deviate by a small amount from an eclipsed configuration when viewed down the metal–O(1) bond. The projection shown is for the nickel adduct; that for the cobalt complex is essentially identical. The torsion angles for the O(3)–M–O(1)–N linkage are 21.4° for M = Ni^{2+} and 19.3° for M = Co^{2+}.

Magnetic Results. Plots of reciprocal molar magnetic susceptibility and effective moment for the cobalt and nickel adducts are shown in Figures 4 and 5, respectively. Complete tables of

(27) Shibaeva, R. N. *J. Struct. Chem.* (*Engl. Transl.*) **1975**, *16*, 318–332 and references therein.
(28) Chion, B.; Lajzerowicz-Bonneteau, J. *Acta Crystallogr., Sect. B: Struct. Crystallogr. Cryst. Chem.* **1980**, *B36*, 998–1000 and references therein.

the magnetic susceptibility data are available as supplementary material.

The effective magnetic moment of the cobalt complex decreases steadily with temperature from its room-temperature value of 3.75 to 2.62 μ_B at 6 K, the lowest temperature investigated. For the nickel adduct, μ_{eff} is 1.51 μ_B at room temperature and decreases with temperature to a constant value of 0.55 ± 0.01 μ_B at $T \leq$ 140 K. Attempts were made to fit the observed susceptibility curves to equations based upon a spin-only interaction Hamiltonian with variable g values and coupling constants and with provision for paramagnetic impurities, but no satisfactory fit could be obtained. More elaborate models, which would of necessity involve more adjustable parameters, were not investigated.

Discussion

This bis(proxyl) adducts of bis(hexafluoroacetylacetonato)cobalt(II) and -nickel(II) are members of a small group of well-characterized compounds that contain two nitroxyl functions bound to a single transition-metal ion. Other examples of such species include the analogous manganese(II) adducts $Mn(F_6acac)_2L_2$ (L = tempo, proxyl),[15] bisadducts of the nitronyl nitroxide nitphen with $CuCl_2$[17] and $Cu(F_6acac)_2$,[19] and a linear-chain copper(II) complex containing a nitroxyl biradical.[29]

The centrosymmetric structure of the two adducts is similar to that reported for bisadducts of unsubstituted cobalt(II) and nickel(II) acetylacetonates with a number of oxygen and nitrogen donor ligands.[30-35] The geometry of the metal coordination sphere, the dimensions of the nitroxyl ligand, and the molecular stoichiometry are consistent with the formulation of both systems as complexes of divalent metal ions with neutral nitroxyl radicals. The magnetic behavior of such a system will depend upon the nature of the interaction between the three paramagnetic centers of the nitroxyl–metal–nitroxyl linkage. The series $M(F_6acac)_2(proxyl)_2$ ($M = Mn^{2+}$, Co^{2+}, Ni^{2+}) provides an unusual example of a set of isostructural species differing only in the identity of the central metal ion. A comparison of the magnetic properties of these systems is clearly of interest.

As is shown in Figure 3, the reciprocal magnetic susceptibility of the Co^{2+} adduct increases steadily with T from about 6 to 250 K and then remains nearly constant from 250 to 300 K. This behavior is indicative of antiferromagnetic coupling, with increasing population of higher spin states as T increases. The effective magnetic moment decreases steadily from 3.76 μ_B at 302 K to 2.62 μ_B at 6 K, the lowest temperature investigated. There is no temperature interval over which μ_{eff} is constant. The low-temperature magnetic moment values indicate that the ground state is a spin doublet. The μ_{eff} value at 6 K, though higher than the spin-only value for $S = {}^1/_2$, is too low for any higher spin ground state. Evidently, there must be a low-lying excited state and/or a small amount of higher spin impurity contributing to the low-temperature susceptibilities. Neither of these affects the qualitative description of the magnetic behavior of this system.

The inverse susceptibility of the nickel adduct increases from 6 K to a maximum at 150 K and then decreases with T. Correspondingly, μ_{eff} decreases from 1.51 μ_B at room temperature to a constant value of 0.55 ± 0.01 μ_B for $T \leq 140$ K. Again, the pattern is one of antiferromagnetic coupling, which in this instance yields a diamagnetic ground state. The small residual low-temperature paramagnetism is probably a consequence of the presence of a small amount of impurity, a common observation in systems like these. We calculate that 1.3% of an impurity with $S = 2$ (i.e., uncomplexed Ni^{2+} and free radicals) would account for the low-temperature paramagnetism.

The qualitative magnetic behavior of these two systems is hence the same as that previously observed for the proxyl and tempo adducts of $Mn(F_6acac)_2$.[15,16] In each case, antiferromagnetic interaction yields a ground state with an S value 1 unit less than that of the corresponding high-spin metal ion. Such a state would most simply be achieved by the coupling of each of the nitroxyl free spins with a metal-based unpaired electron. In the case of the manganese adducts, fitting of the experimental susceptibility curve to a spin-only theoretical expression including only nearest-neighbor interaction terms yielded values for the coupling constants and a quantitative energy level scheme. Although this was not achieved for the cobalt or nickel systems, the qualitative magnetic behavior of these adducts indicates antiferromagnetic interactions of the same order of magnitude as those in the manganese complexes.

The unpaired electron in a free nitroxyl radical occupies an orbital of π^* symmetry with respect to the N–O bond. Antiferromagnetic coupling requires nonzero overlap of this orbital with one or more of the magnetic orbitals of the metal ion.[36] Metal orbitals of appropriate symmetry for such an interaction include the d_{z^2}, d_{xz}, and $d_{x^2-y^2}$ orbitals.[37] For the previously reported bis(nitroxyl) adducts of Mn^{2+}, all three of these would contain unpaired electrons. In the nickel complex, however, only the d_{z^2} and $d_{x^2-y^2}$ metal orbitals are likely to be singly occupied. Although overlap of the nitroxyl π^* orbital with the d_{z^2} orbital would presumably be greater than that with the $d_{x^2-y^2}$ orbital, both interactions must be invoked to account for the diamagnetic ground state of the nickel adduct. Investigation of the magnetic properties of an isostructural complex of a d^9 metal ion could yield additional information about the π^*–$d_{x^2-y^2}$ interaction; however, it has not yet proven to be possible to prepare the appropriate adducts.

In summary, the temperature dependence of the magnetic susceptibilities of the bis(proxyl) adducts of cobalt(II) and nickel(II) hexafluoroacetylacetonates implies antiferromagnetic coupling of metal and ligand free spins, with $S = {}^1/_2$ ($M = Co^{2+}$) and $S = 0$ ($M = Ni^{2+}$) ground states. The effects of population of higher spin excited states are also seen. This interpretation is similar to that previously offered for two isostructural manganese(II) adducts. Plausible orbital overlap interactions that account for this behavior can be identified.

Acknowledgment. Access to the Cambridge Structural Database was obtained through the San Diego Supercomputer Center, supported by the National Science Foundation. The SQUID magnetometer at the University of Southern California was purchased with the aid of a grant from the National Science Foundation.

Registry No. $Ni(F_6acac)_2(proxyl)_2$, 113220-37-4; $Co(F_6acac)_2(proxyl)_2$, 113220-38-5; $Co(F_6acac)_2$, 19648-83-0; $Ni(F_6acac)_2$, 14949-69-0.

Supplementary Material Available: Tables of anisotropic thermal parameters, hydrogen atom coordinates, distances and angles within the CF_3 groups, least-squares planes, and magnetic susceptibility data (9 pages); tables of calculated and observed structure factors (14 pages). Ordering information is given on any current masthead page.

(29) Matsunaga, P.; Carducci, M.; Doedens, R. J., unpublished work.
(30) Bullen, G. J. *Acta Crystallogr.* **1959**, *12*, 703–708.
(31) Montgomery, H.; Lingafelter, E. C. *Acta Crystallogr.* **1964**, *17*, 1481–1482.
(32) Elder, R. C. *Inorg. Chem.* **1968**, *7*, 1117–1123.
(33) Elder, R. C. *Inorg. Chem.* **1968**, *7*, 2316–2322.
(34) Pfluger, C. E.; Burke, T. S.; Bednowitz, A. L. *J. Cryst. Mol. Struct.* **1973**, *3*, 181–191.
(35) Hursthouse, M. B.; Malik, K. M. A.; Davies, J. E.; Harding, J. H. *Acta Crystallogr., Sect. B: Struct. Crystallogr. Cryst. Chem.* **1978**, *B34*, 1355–1357.
(36) See, for example: *Magneto-Structural Correlations in Exchange Coupled Systems*; Willett, R. D., Gatteschi, D., Kahn, O., Eds.; D. Reidel: Dordrecht, Holland, 1985.
(37) Designations of metal atomic orbitals are referred to a Cartesian coordinate system with z lying along the metal–O(nitroxyl) bond and with the N–O bond lying in the xz plane. Although the rigorous site symmetry at the metal atom is only C_i, the deviation from octahedral symmetry is not great. Consequently, an octahedral energy level pattern is a reasonable starting point in a discussion of the orbital interactions in these compounds.